

Fundamental building blocks for molecular biowire based forward error-correcting biosensors

This article has been downloaded from IOPscience. Please scroll down to see the full text article.

2007 Nanotechnology 18 424017

(<http://iopscience.iop.org/0957-4484/18/42/424017>)

View [the table of contents for this issue](#), or go to the [journal homepage](#) for more

Download details:

IP Address: 35.9.138.193

The article was downloaded on 01/12/2010 at 19:55

Please note that [terms and conditions apply](#).

Fundamental building blocks for molecular biowire based forward error-correcting biosensors

Yang Liu¹, Shantanu Chakrabartty¹ and Evangelyn C Alocilja²

¹ Electrical and Computer Engineering, Michigan State University, East Lansing, MI 48824, USA

² Biosystems Engineering, Michigan State University, East Lansing, MI 48824, USA

E-mail: liuyang4@egr.msu.edu

Received 3 April 2007, in final form 14 July 2007

Published 19 September 2007

Online at stacks.iop.org/Nano/18/424017

Abstract

This paper describes the fabrication, characterization and modeling of fundamental logic gates that can be used for designing biosensors with embedded forward error-correction (FEC). The proposed logic gates (AND and OR) are constructed by patterning antibodies at different spatial locations along the substrate of a lateral flow immunosensor assay. The logic gates operate by converting binding events between an antigen and an antibody into a measurable electrical signal using polyaniline nanowires as the transducer. In this study, *B. cereus* and *E. coli* have been chosen as model pathogens. The functionality of the AND and OR logic gates has been validated using conductance measurements with different pathogen concentrations. Experimental results show that the change in conductance across the gates can be modeled as a log-linear response with respect to varying pathogen concentration. Equivalent circuits models for AND and OR logic gates have been derived based on measured results.

(Some figures in this article are in colour only in the electronic version)

1. Introduction

Every year approximately 5000 deaths in the United States are attributed to disease outbreaks due to food-borne pathogens [1, 2]. The United States Department of Agriculture (USDA) estimate indicates a loss of \$2.9–\$6.7 billion due to medical costs and lost productivity because of these outbreaks [2–6]. Biosensors have emerged as important analytical tools for the rapid detection of pathogens in the field, and thus they play a key role in controlling disease outbreaks. Biosensors, typically, possess biological recognition elements as a reactive surface in close proximity to a transducer, which converts the binding of an analyte with the biological recognition layer into a measurable electrical or optical signal [7, 8]. Immunosensors (biosensors that use antibodies as biological recognition elements) are of great interest because of their applicability (any compound can be analyzed as long as specific antibodies are available) and high sensitivity. In particular, immunosensors with electrical readouts offer

several advantages over their optical counterparts due to their reduced cost, reduced form factor and ease of signal acquisition. One such immunosensor, which is used in this study, was introduced in [9–11], and it has been shown to achieve a detection limit of 80 colony forming units (CFU)/ml for bacteria and 10^3 cell culture infective dose per milliliter (CCID/ml) of bovine viral diarrhoea virus (BVDV) antigens in approximately 6 min. The immunosensor uses conductive polyaniline as a transducer and a molecular switch which is triggered by presence of target pathogen in the analyte. The use of polyaniline as a switch (yielding ‘on’ and ‘off’ responses) has previously been demonstrated using dual gold film electrodes [12]. In some biosensor configurations, polyaniline has also been used as an amplifier to improve the detection process [13, 14]. Conductive polyaniline nanowire based immunosensors are relatively inexpensive to fabricate and easy to operate, which makes them an ideal candidate for multi-array biosensor architecture that can achieve reliable detection of pathogens. Reliable detection of pathogens at

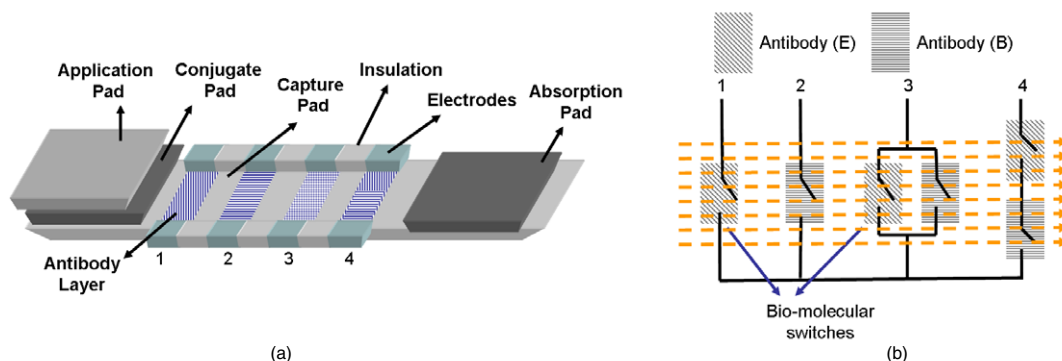


Figure 1. (a) Visualization of the final multi-array biosensor prototype. (b) Logical model of the prototype based on fundamental AND and OR operations.

low concentration levels is especially important for certain pathogens (also referred to as zero-tolerance pathogens) where trace quantities have been shown to be dangerous for human ingestion. For instance, the US Food Safety and Inspection Service (FSIS) has established a zero tolerance threshold for *E. coli* O157:H7 contamination in raw meat products [15]. The infectious dosage of *E. coli* O157:H7 is ten cells; the Environmental Protection Agency (EPA) standard in water is 40 cells per liter [6]. The US also has a zero tolerance rule for *Salmonella*, *L. monocytogenes* [6, 16, 17]. In our previous study, a machine learning approach was used to improve the detection rate of multiple pathogens at low concentration levels [18] with error rates less than 2% for concentrations ranging from 10^0 to 10^7 CFU/ml. However, a major disadvantage of the approach is the requirement of a large calibration dataset for training a reliable learning model.

Although high sensitivity is an important attribute in designing biosensors, a large variance due to stochastic interaction between biomolecules, biosensor imperfections, environmental variability (e.g., pH of the analyte) directly affects the reliability of the measured signal. One of the methods for compensating sensor level imperfections is by use of forward error-correction (FEC) techniques. FEC principles have been successfully applied in improving the reliability of devices (for example in compact disks) whereby redundancy is introduced during the fabrication process such that any occurrence of errors due to device imperfections can be corrected. In fact, biological phenomena that are prone to stochastic artefacts have been shown to also use FEC principles for improving the reliability [19, 20].

In this paper we present the implementation (fabrication, characterization and modeling) of fundamental building blocks that will implement FEC on the polyaniline based immunosensor. These building blocks will include specialized logic gates (AND and OR) that will operate based on specific binding between antigen and antibodies. In the literature several studies have been reported in the area of biomolecular computing [21–24], that use biological entities (DNA, single molecules) for performing logical functions. However, in this work the integration of computation and sensing functions within each logic gate serves as an ideal candidate for implementing biosensor error correction. The paper is organized as follows. Section 2 describes the architecture of a multi-array immunosensor and its principle of

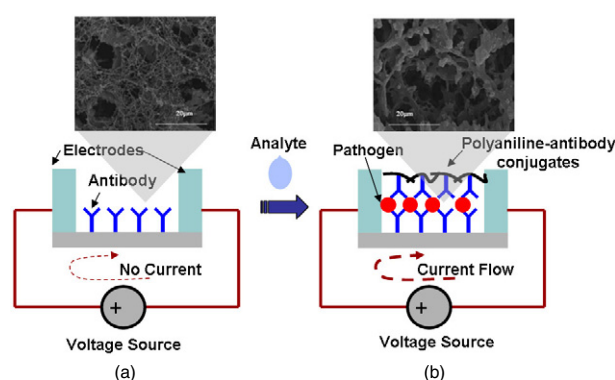


Figure 2. Illustration of principle of operation of a single pathogen biosensor: cross-section of the capture pad (schematic and SEM) (a) before and (b) after application of the analyte.

operation. Section 3 presents the material preparation methods used for constructing the fundamental logic gates; section 4 presents experimental results using the fabricated prototype and introduces an equivalent circuit model for the logic gates. Finally, conclusions are given and future work is described in section 5.

2. System architecture and principle of operation

The architecture of a multi-array forward error-correcting biosensor is shown in figure 1(a). It is composed of four different pads: sample application, conjugate, capture, and absorption pads. By patterning the antibodies along different spatial locations on the capture pad, basic logic gates (AND/OR) can be implemented. Figure 1(b) shows the logical model for the multi-array biosensor shown in figure 1(a). Each antibody region will constitute a biomolecular switch triggered by specific antigens present in the analyte. As an example, region 3 in figure 1(b) is formed by mixing two antibodies together, thus forming an OR logic gate. Similarly, region 4 in figure 1(b) constitutes a cascade of two switches which forms an AND logic gate.

The principle of operation of a single biomolecular switch is illustrated in figures 2(a) and (b), which show a cross-sectional view of the immunosensor. Before the sample is applied, the gap between the electrodes in the capture

pad is open (figure 2(a)). Immediately after the sample is applied to the application pad, the solution containing the antigen flows to the conjugate pad, dissolves with the polyaniline-labeled antibody (Ab-P) and forms an antigen-antibody-polyaniline complex. The complex is transported using capillary action into the capture pad containing the immobilized antibodies. A second antibody-antigen reaction occurs and forms a sandwich (figure 2(b)). The polyaniline in the sandwich then forms a molecular wire and bridges the two electrodes. The polymer structures extend out to bridge adjacent cells and leads to an impedance change between the electrodes [14]. The impedance change is determined by the number of antigen-antibody bindings, which is related to the antigen concentration in the sample. The unbound non-target organisms are subsequently separated by capillary flow to the absorption membrane. The impedance change is sensed as an electrical signal (current) across the electrodes. In figures 2(a) and (b) we show scanning electron microscope (SEM) images of the capture pad before and after the analyte with pathogen has been applied. The change in material texture can be observed in figure 2(b); this is attributed to the formation of the antibody-antigen-antibody-polyaniline complex connecting the electrodes.

3. Material preparation and methods

3.1. Biosensor preparation

Purified rabbit polyclonal antibodies against *B. cereus* and *E. coli* were obtained from Biodesign International (Saco, ME, USA). The antibodies were suspended in phosphate buffer solution (pH 7.4) upon receipt and stored at 4 °C. *B. cereus* and *E. coli* strains were obtained from the National Food Safety and Toxicology Center (Michigan State University) and the Michigan Department of Community Health (East Lansing, MI, USA). A 10 μ l loop of each isolate was cultured in 10 ml of nutrient broth and incubated for 24 h at 37 °C to prepare stock cultures. The stock cultures were serially diluted with 0.1% peptone water to obtain varying concentrations of each microorganism. Polyaniline was purchased from Sigma-Aldrich (St Louis, MO, USA). All experiments were carried out in a certified Biological Safety Label II laboratory.

The application sample pads (size: 15 mm \times 5 mm) and absorption pads (size: 20 mm \times 5 mm) were made of nitrocellulose membrane (flow rate: 135 s/4 cm) and the conjugate pads (size: 10 mm \times 5 mm) were made of fiberglass membrane (grade G6). The porous nitrocellulose substrate ensures good adsorption properties for immobilized antibodies and allows non-target antigens to flow through. The electrodes were fabricated with silver paste and they provided electrical connection between the nitrocellulose membrane and a data acquisition system. The conjugate pad was designed to allow maximal adsorption and flow of polyaniline-conjugated antibodies. The antibody concentration used for the conjugate pad was 150 μ g ml⁻¹ and for the capture pad it was 500 μ g ml⁻¹. The polyaniline concentration in the conjugate pad was 1 mg ml⁻¹. All these values were found to be optimal, resulting in the highest ratio between the number of captured cells and the actual cell concentration tested [10]. The immunosensors were attached to an etched copper printed circuit board (PCB) which was used to connect to the data

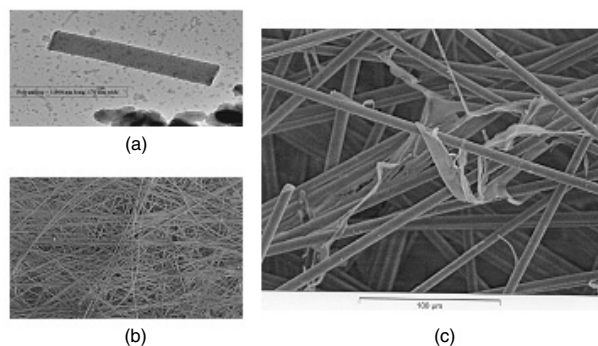


Figure 3. (a) synthesized polyaniline, (b) polyaniline nanowire bundles, and (c) a polyaniline nanowire functionalized with antibodies.

acquisition system. For signal measurement, the prepared biosensor was connected to a BK multimeter Model AK-2880A (Worcester, MA, USA) with the RS-232 interface and BK software. The signal measured by the multimeter was in the form of change in resistance.

3.2. Fabrication and characterization of AND and OR logic gates

The polyaniline-multi-variate antibody (PMA) conjugates were prepared by suspending 800 μ l of polyclonal antibodies against *B. cereus* and *E. coli* (concentration 150 μ g ml⁻¹) in 4 ml of polyaniline solution in phosphate buffer (pH 7.4) containing 10% dimethylformamide (DMF) (v/v) and 1% LiCl (w/v). The solution was incubated at room temperature for 1 h to allow binding of the antibodies with the polyaniline and then treated with a blocking reagent (Tris buffer containing 0.1% casein). The polyaniline-multi-variate antibody conjugates were then precipitated by centrifugation at 12 000 rpm for 5 min. The supernatant fluid was discarded and the pellets were mixed with the blocking reagent and centrifuged again. The centrifugation step was repeated three times. The conjugates were finally suspended in phosphate buffer solution containing 1% LiCl (w/v) and 10% DMF (v/v) and stored at 4 °C until use. The conjugate pads were prepared by soaking the fiberglass strip into the PMA solution until homogenous dispersion was achieved. Figure 3 shows an SEM image of: (a) synthesized polyaniline (diameter 170 nm); (b) polyaniline nanowire bundles; and (c) a polyaniline nanowire functionalized with antibodies.

For preparing the OR gates on the capture pad, a mixture of polyclonal antibodies against *B. cereus* and *E. coli* (concentration 500 μ g ml⁻¹) was dispensed onto the surface of the capture pad. AND gates were fabricated on the capture pad by using a mask to isolate *B. cereus* and *E. coli* antibodies, which leads to a cascaded pattern (shown in figure 1(a): region 4). The logic gates were characterized to determine their variations due to different concentration of pathogens. Pure cultures of *B. cereus* and *E. coli* were serially diluted five times using 9 ml of 0.1% (v/v) peptone water to prepare ten-fold dilutions representing cell concentrations ranging from 10² to 10⁶ CFU/ml. Each of the tests was repeated three times and the results were measured 6 min after the application of the

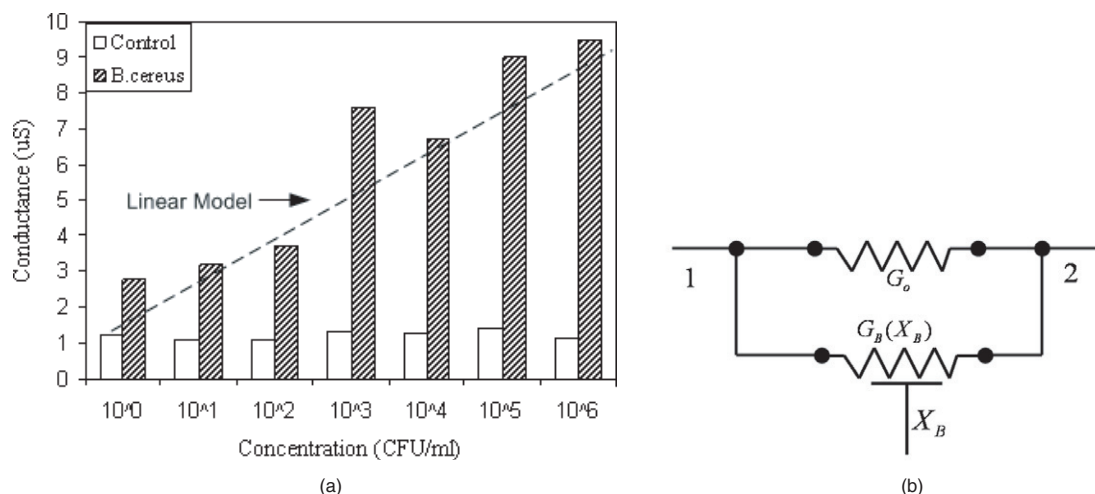


Figure 4. (a) Conductance measured across the electrodes of a *B. cereus* biosensor for different pathogen concentrations; (b) an equivalent circuit model for the single pathogen immunosensor.

analyte. ‘Control’ for all the experiments was obtained using blank peptone water.

4. Results and discussions

4.1. Characterization of a single pathogen biosensor

For the first set of measurements, a *B. cereus* immunosensor was fabricated based on the procedure described in section 3. The conductance across the electrodes was measured for analytes with different pathogen concentrations. A typical response of the biosensor constitutes a varying conductance for approximately 1 min after which the measurement stabilizes. This variation is attributed to the typical settling behavior of the polyaniline sandwich in the presence of the lateral flow, adhesion and capillary force. Figure 4(a) shows the measured conductance as the pathogen concentration is varied. The conductance is plotted against the ‘control’ measurement (response of the biosensor when no pathogen is present) showing clear discrimination between pathogenic and non-pathogenic cases. The plot also shows an increase in conductance with increase in concentration with sources of error arising due to imprecise patterning of the electrodes. A first-order response of the biosensor with respect to varying concentration can be approximated by a log-linear model (shown by the dashed line in figure 4(a)) and is given by

$$G(X_B) = G_0 + \kappa_B \log_{10} \left(\frac{X_B}{X_0} \right) \quad (1)$$

where X_B represents the concentration of the pathogen (*B. cereus*) in CFU/ml, G_0 represents the ‘control’ transconductance, κ_B represents a sensitivity factor and X_0 is a detection constant. Note that equation (1) is valid only for $X_B > X_0$, which is a reasonable assumption.

An equivalent circuit model based on equation (1) is shown in figure 4(b), which depicts a ‘concentration’ controlled resistor whose operation has equivalence to a transistor. Therefore the device in figure 4(b) can be considered as a ‘biomolecular transistor’. In fact, equation (1) can

be shown to be equivalent to the sub-threshold response of a metal–oxide–semiconductor (MOS) transistor [25]. The typical values of parameters in equation (1) as calculated from figure 4(a) are $G_0 = 1.24 \mu\text{S}$, $\kappa_B = 1.2 \mu\text{S}$ and $X_0 = 10^{-1}$ CFU/ml. Limitations of the log-linear model in equation (1) in predicting the pathogen concentration will arise due to the ‘hook effect’, a common phenomenon observed in most biosensors where the conductance decreases with increase in pathogen concentration. The ‘hook effect’ is typically attributed to the presence of a large concentration of pathogens, leading to saturation of binding sites and obstructing charge transfer within the conductive polyaniline structure. For instance, in [10] the ‘hook effect’ was observed at concentrations above 10^4 CFU/ml for a biosensor electrode spacing of approximately 0.5 mm. In our experiments, the electrodes are spaced approximately at 1 mm, and therefore the ‘hook effect’ was not observed, possibly at the expense of reduced sensitivity factor κ_B .

4.2. Characterization of AND and OR logic gates

For the next set of experiments, polyclonal anti-*B. cereus* and anti-*E. coli* were used to fabricate OR and AND gates using the procedure described in section 3. Figure 5(a) shows the response of an AND gate corresponding to two pathogens: *E. coli* and *B. cereus*. The conductance of the immunosensor was measured for two sets of pathogen concentration and for four possible logic conditions ($E = \{0, 1\}$ and $B = \{0, 1\}$) where a binary state represents the absence or presence of a pathogen. The measured conductance was compared against a ‘control’ response which represents the logic condition $E = 0, B = 0$. It can be seen from figure 5(a) that the measured conductance for the logical condition ($E = 1, B = 1$) is higher than all other cases (irrespective of pathogen concentration), which corresponds to a true AND operation. However, figure 5(a) also shows that the measured conductance when only *B. cereus* is present is close to the condition when both *B. cereus* and *E. coli* are present. This artefact could be attributed to the imperfect

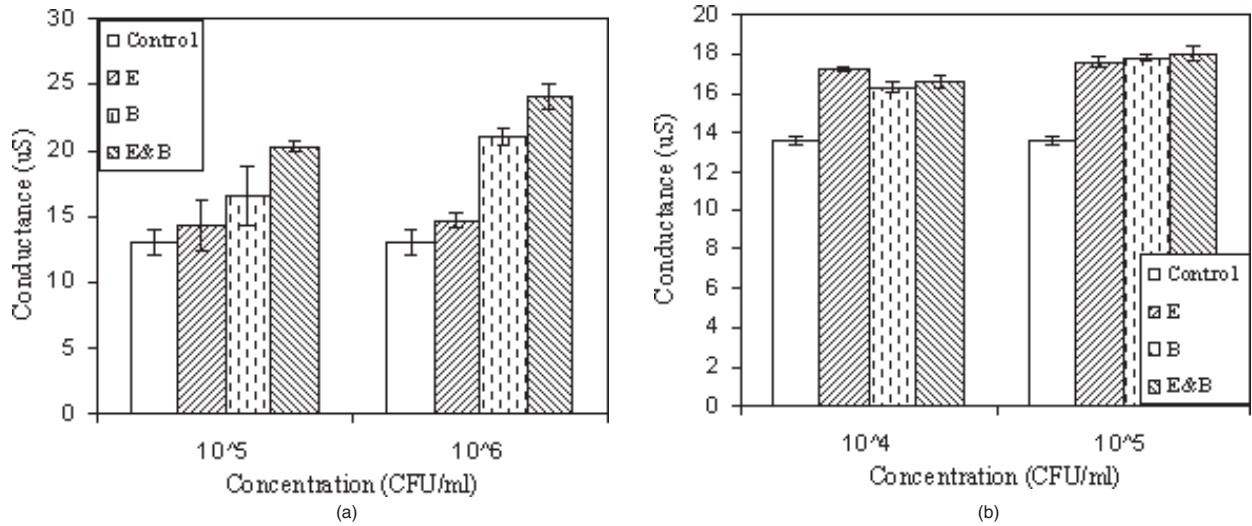


Figure 5. Conductance measurements obtained from a two-pathogen biosensor (*B. cereus*, *E. coli*) configured for (a) AND operation and (b) OR operation.

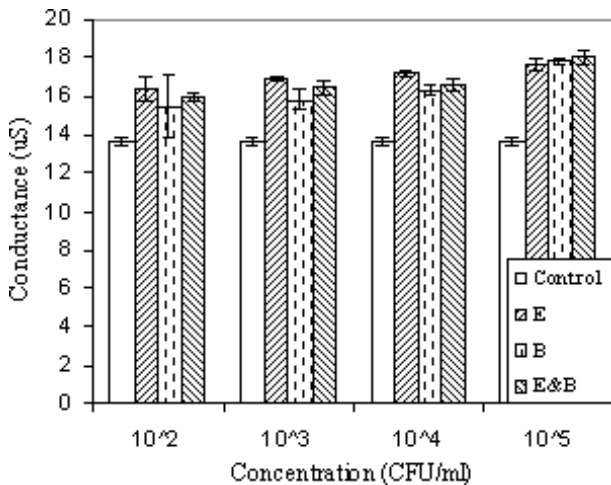


Figure 6. Conductance measurements obtained from a two-pathogen biosensor (*B. cereus*, *E. coli*) configured as an OR logic for four different bacterial concentrations.

antibody masking in the fabrication procedure which led to signal leakage across the electrodes. Figure 5(b) shows the measured conductance for a biosensor acting as an OR logic gate. The plot shows that, for both pathogen concentration levels, the ‘control’ condition ($E = 0, B = 0$) leads to a lower conductance as compared to other logical states. Therefore the response of the biosensor is equivalent to an OR logic. Also note that OR logic is easy to pattern (no masking required), therefore leading to near ideal operation as compared to an equivalent AND gate.

Figure 6 plots the response of an OR gate for four different pathogen concentration levels. The results indicate that OR operation is consistent across different concentration levels of pathogen. Also note that the response for different logic conditions exhibits a log-linear response similar to equation (1). This behavior is modeled by its equivalent circuit shown in figure 7(a). The circuit is similar to a ‘pass-transistor’ logic, where the ‘biomolecular transistors’ are connected in

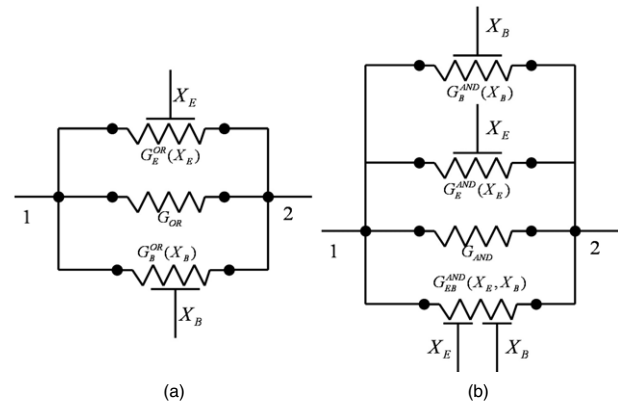


Figure 7. Circuit model for (a) an OR gate formed by a two-pathogen biosensor and (b) an AND gate formed by a two-pathogen biosensor.

parallel. The conductance measured across the OR gate can be modeled as a function of *B. cereus* and *E. coli* concentrations (X_B, X_E) as

$$G(X_B, X_E) = G_{OR} + \kappa_B^{OR} \log_{10} \left(\frac{X_B}{X_{0B}^{OR}} \right) + \kappa_E^{OR} \log_{10} \left(\frac{X_E}{X_{0E}^{OR}} \right) \quad (2)$$

where $G_{OR}, \kappa_B^{OR}, \kappa_E^{OR}, X_{0E}^{OR}, X_{0B}^{OR}$ represent ‘control transconductance’, sensitivity factors and detection constants for *B. cereus* and *E. coli* in the OR configuration. These constants are calculated using measured results with the regression procedure described in section 4.1. Typical values of these constants are given in table 1.

Similarly, the response of an AND gate is modeled according to the relation

$$G(X_B, X_E) = G_{AND} + \kappa_B^{AND} \log_{10} \left(\frac{X_B}{X_{0B}^{AND}} \right) + \kappa_E^{AND} \log_{10} \left(\frac{X_E}{X_{0E}^{AND}} \right) + \kappa_{EB}^{AND} \log_{10} \left(\frac{X_E + X_B}{X_{0EB}^{AND}} \right) \quad (3)$$

Table 1. Parameters of OR and AND circuit model in figure 7.

OR		AND	
Parameter	Value	Parameter	Value
G_{OR}	13.6 μ S	G_{AND}	13.1 μ S
κ_B^{OR}	0.15 μ S	κ_B^{AND}	3.4 μ S
X_{OB}^{OR}	0.76 CFU/ml	X_{OB}^{AND}	10 ³ CFU/ml
κ_E^{OR}	0.09 μ S	κ_E^{AND}	0.45 μ S
X_{OE}^{OR}	8.5 $\times 10^{-4}$ CFU/ml	X_{OE}^{AND}	4.6 $\times 10^2$ CFU/ml
		κ_{EB}^{AND}	0.4 μ S
		X_{OEB}^{AND}	1.2 $\times 10^3$ CFU/ml

where the constants κ_{OEB}^{AND} , X_{OEB}^{AND} model the coupling between *E. coli* and *B. cereus* pathogens to produce an AND response. The parameters of the AND gate calculated from the measured results are summarized in table 1. Note that for an ideal AND operation $\kappa_{OEB}^{AND} \gg \kappa_{OB}^{AND}, \kappa_{OE}^{AND}$. However, from the results it can be seen that the AND gate response is far from ideal, but it does satisfy $\kappa_{OEB}^{AND} > \kappa_{OB}^{AND}, \kappa_{OE}^{AND}$. Future work will focus on improving the masking process for fabricating AND gates.

5. Conclusions and future work

In this paper we have shown the feasibility of constructing basic logic gates (AND and OR) on a lateral flow immunosensor. AND logic gates have been constructed by cascading *B. cereus* and *E. coli* antibodies, whereas OR logic gates have been fabricated by homogeneously mixing and dispensing of antibodies. The immunosensor logic gates utilize conductive polyaniline nanowire as the transducer in conjunction with specific antigen–antibody binding. The functionality of the AND and OR logic gates has been validated using conductance measurements for different pathogen concentrations. Experimental results show that the change in conductance across the gates can be modeled using a log-linear response with respect to varying pathogen concentration. Equivalent circuit models for AND and OR logic gates have been presented and the model parameters have been calculated using measured results. The proposed logic gates and their circuit models will play a fundamental role in designing a multi-array ‘computational biosensor’ that will embed error-control codes within its sensor structure. Forward error-correction on the ‘computational biosensor’ will be able to correct detection errors introduced by environmental variations, non-specific antigen–antibody binding and structural artefacts.

Acknowledgments

This work is supported by a research grant from the National Science Foundation: NSF ECCS-0622056. The authors would like to thank Sudeshna Pal for providing assistance in preparing the immunosensors.

References

- [1] Young G O 1964 Synthetic structure of industrial plastics *Plastics* 2nd edn, vol 3, ed J Peters (New York: McGraw-Hill) pp 15–64

- [2] Mead P, Slutsker L, Dietz V, McCaig L, Breese J, Shapiro S, Griffin P and Tauxe R 1999 Food-related illness and death in the United States *Emerg. Infect. Dis.* **5** 607–25
- [3] Radke S M and Alocilja E C 2005 A microfabricated biosensor for detecting foodborne bioterrorism agents *IEEE Sensors J.* **5** 744–50
- [4] Rainford C 2004 NEWS: US farm income expected down \$5.5 billion in 2004 *Agricult.* Online available: <http://www.agriculture.com/AgNews.class>
- [5] *Food and Drug Administration, Bacteriological Analytical Manual* 2000 8th edn (Arlington, VA: Association of Analytical Chemists)
- [6] Dubovi E J 1990 The diagnosis of bovine viral diarrhoea virus—A laboratory view *Vet. Med.* **85** 1133–9
- [7] Ivnitski D, Abdel-Hamid I, Atanasov P and Wilkins E 1999 Biosensor for detection of pathogenic bacteria *Biosens. Bioelectron.* **14** 599–624
- [8] Cahn T M 1993 *Biosensors* (London: Chapman and Hall)
- [9] Muhammad-Tahir Z and Alocilja E C 2003 A conductimetric biosensor for biosecurity *Biosens. Bioelectron.* **18** 813–9
- [10] Muhammad-Tahir Z and Alocilja E C 2003 Fabrication of a disposable biosensor for *Escherichia coli* o157:H7 detection *IEEE Sensors J.* **3** 345–51
- [11] Muhammad-Tahir Z, Alocilja E C and Grooms D L 2005 Rapid detection of bovine viral diarrhoea virus as surrogate of bioterrorism agents *IEEE Sensors J.* **5** 757–62
- [12] Iribe Y and Suzuki M 2002 Integrated enzyme switch as a novel biosensing device *Biosensors and Bioelectronics, The 7th World Congress of Biosensors (Japan)*
- [13] Sergeeva T A, Piletskii S A, Rachkov A E and El'Skaya A V 1996 Polyaniline label-based conductometric sensor for IgG detection *Sensors Actuators B* **34** 283–8
- [14] Kim J H, Cho J H and Cha G S 2000 Conductimetric membrane strip immunosensor with polyaniline bound gold colloids as signal generator *Biosens. Bioelectron.* **14** 907–15
- [15] Jay J M 2000 *Modern Food Microbiology* (Gaithersburg, MD: Aspen Publishers)
- [16] Ryser E T 1998 Public Health Concerns *Applied Dairy Microbiology* ed E H Marth and J L Steele (New York: Dekker) pp 263–404
- [17] Jones G M 1999 Testing bulk tank milk samples <http://www.ext.vt.edu/pubs/dairy/404-405/404-405.htm>
- [18] Zuo Y, Chakrabarty S, Muhammad-Tahir Z, Pal S and Alocilja E C 2006 Spatio-temporal processing for multichannel biosensors using support vector machines *IEEE Sensors J.* **1644–51**
- [19] Fedichkin L, Katz E and Privman V 2007 Error correction and digitalization concepts in biochemical computing *J. Comput. Theor. Nanosci.* at press (Fedichkin L, Katz E and Privman V 2007 *Preprint cond-mat/0703351*)
- [20] May E E, Johnston A M, Hart W E, Watson J, Pryor R J and Rintoul M D 2003 Detection and reconstruction of error control codes for engineered and biological regulatory systems *SAND Report* Sandia National Laboratories pp 2003–3963
- [21] Seelig G, Soloveichik D, Zhang D Y and Winfree E 2006 Enzyme-free nucleic acid logic circuits *Science* **314** 1585–8
- [22] Magri D C, Brown G J, McClean G D and Prasanna de Silva A 2006 Communicating chemical congregation: a molecular AND logic gate with three chemical inputs as a ‘lab-on-a-molecule’ prototype *J. Am. Chem. Soc.* **128** 4950–1
- [23] Margulies D, Melman G and Shanzer A 2006 A molecular full-adder and full-subtractor, an additional step toward a molecular *J. Am. Chem. Soc.* **128** 4865–71
- [24] Stadler R, Ami S, Joachim C and Forshaw M 2004 Integrating logic functions inside a single molecule *Nanotechnology* **15** S115–21
- [25] Mead C 1989 *Analog VLSI and Neural Systems* (Reading, MA: Addison-Wesley)